Dynamic Voltage Control of Converters with LC-filters Using Model Predictive Control: Impacts on Grid-Forming and Grid-Following Control

Author(s):
Jeong, Min; Biela, Jürgen

Publication date:
2023

Permanent link:
https://doi.org/10.3929/ethz-b-000612200

Originally published in:
https://doi.org/10.23919/ICPE2023-ECCEAsia54778.2023.10213610

Dynamic Voltage Control of Converters with *LC*-filters Using Model Predictive Control: Impacts on Grid-Forming and Grid-Following Control

Min Jeong
High Power Electronic Systems (HPE)
ETH Zürich
jeong@hpe.ee.ethz.ch

Jürgen Biela
High Power Electronic Systems (HPE)
ETH Zürich
jbiela@ethz.ch

***Abstract*—Conventional multi-loop controllers for voltage control of converters with LC-filters usually have a limited control bandwidth due to resonances. However, when model predictive control (MPC) with a long-prediction horizon is applied, dynamic voltage control with an excellent damping behavior can be achieved. This enables VSCs with LC-filters to closely match the behavior of ideal controllable voltage sources, which are desirable for grid-forming and grid-following control. In this paper, the impact of dynamic voltage control using MPC on such grid-forming and grid-following control is analysed, and simulation results are presented to validate the analysis.**

***Index Terms*—Continuous control set (CCS) MPC, Indirect MPC, Droop control, Current limitation, Power oscillation**

I. Introduction

Voltage-source converters (VSCs) are widely used to integrate distributed power sources into the power grid. The VSCs have been typically connected to the grid as grid-following converters (GFLCs), which are controlled as current sources assuming that the power grid is stiffly formed [1], [2]. GFLCs regulate injected current levels based on current references from power control loops and grid angles determined by phase-locked loops (PLLs). Currently, the assumed stiff power grid is mostly supported/stabilised by centralized synchronous generators (SGs) to maintain the required voltage and frequency. However, the increasing share of renewable energy sources is fundamentally changing the grid operation, and the VSCs are gradually required to operate as grid-forming units to regulate the system voltage/frequency and emulate the inertia which is usually provided by SGs [3], [4]. There, grid-forming converters (GFMCs) are controlled as voltage sources.

A typical three-phase two-level converter topology operating either as GFLC or GFMC is shown in fig. 1, where an LC-filter is attached to the VSC and is connected to the grid at the point of common coupling (PCC) via inductors L_g, which partly can be realised by the line inductance. When the VSC operates as a GFMC, the filter capacitor voltage v_fc is regulated to track a voltage amplitude V and a phase angle θ reference, i.e. the reference voltage is $v_\mathrm{fc}^* = V\angle\theta$. Ideally, the VSC with the LC-filter is expected to behave as a controllable voltage source.

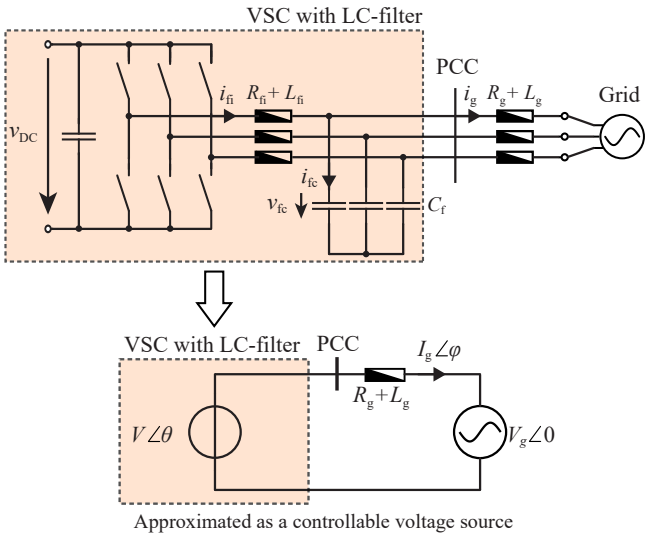

Fig. 1. Three-phase two-level VSC with LC-filters connected to the grid at the PCC and its equivalent per-phase phasor model with an approximated controllable voltage source.

Often multi-loop controllers are used for voltage control as shown in fig. 2(a), which have a cascaded structure including an outer voltage control loop and an inner current control loop [1], [2]. The current loop helps to damp the LC-resonance for enhancing the system stability and to limit over-currents in the system. However, the achievable control bandwidth of multi-loop control methods for approximately acting as a controllable voltage source is very limited due to the LC-filter resonance [4]. Since the active power P and the reactive power Q loops in the power control loop are coupled, the dynamic behavior of the voltage control to follow the references (V, θ) determined by the power control loop is critical for avoiding a coupling of the power control and power oscillations [3]. Furthermore, with the integration of renewable energy resources, new grid operating conditions arises, which require higher power loop bandwidths [5]. Examples of such conditions are microgrids and distributed generations with small capacities and low droop coefficients. This can further challenge power control dynamics and the stability of the operation of GFMCs.

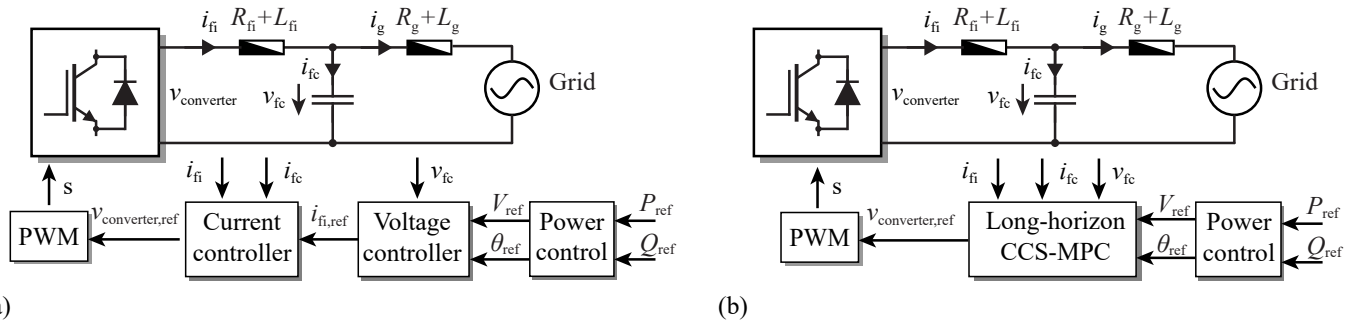

Fig. 2. Voltage control schemes in VSCs with LC-filters. (a) Multi-loop control, which has a limited control bandwidth with poor LC-resonance damping behaviors. (b) Long-horizon CCS-MPC (LHCCS-MPC), which has fast and damped control behaviors considering constraints.

Many MPC concepts have been proposed for controlling the capacitor output voltage of VSCs with LC-filters [6], [7], but most of the attempts are limited to short prediction horizons and therefore cannot fully exploit the inherent damping capability of MPC. Similar to predicting the resonance of an LCL-filter for the current control in [8], the resonance of the LC-filter can be predicted when MPC with a long-prediction horizon is applied for voltage control. Such an MPC can achieve a dynamic control behavior with sufficient damping without extra passive components or additional damping loops.

This paper demonstrates a dynamic voltage control with a high control bandwidth and sufficient damping based on MPC and investigates the impact of MPC on the operation of GFMCs and GFLCs. MPC can also include current limits as control constraints to avoid overcurrents in the system. Since MPC inherently includes the constraints in the controller without extra control loops, problems occurring in conventional controllers can be avoided, which includes latch/wind-up issues and mode changes [9]. Lastly, since VSCs with LC-filters using MPC can closely match the behavior of ideal controllable voltage sources, such a system could be modeled as a controllable voltage source connected to the grid through a simple L-filter. This allows a grid-side current control similar to a L-filter current control, which avoids all control complexities due to resonances and enhances the control robustness under varying grid impedance conditions. Note that an additional MPC for the outer L-filter current control does not bring substantial benefits as the L-filter is a simple first-order system.

This paper is organised as follows: First, the used MPC for the voltage control of VSCs with LC-filters is explained in section II. Section III presents the impact of MPC on GFMCs. Section IV investigates the impact of MPC on GFLCs before concluding in section V.

II. Long-horizon CCS-MPC for Voltage Control

In this paper, a long-horizon continuous control set MPC (LHCCS-MPC) is used similar to the MPC proposed in [10]. However, since the control objective is changed from grid currents to filter capacitor voltages, the differences between filter capacitor voltages and their references are penalised by modifying the weighting matrices in the cost function. Furthermore, state constraints for the converter-side inductor currents are included to protect damage of VSCs caused by overcurrents.

Based on these assumptions, the MPC law can be formulated as

$$\min_{\mathbf{U}_k} \sum_{l=0}^{N_p-1} \left\|\mathbf{x}_{k+l+1} - \mathbf{x}_{ref,k+l+1}\right\|^2_{\mathbf{Q}} + \left\|\mathbf{u}_{k+l} - \mathbf{u}_{k+l-1}\right\|^2_{\mathbf{R}}$$

$$s.t. \quad \mathbf{x}_{k+l+1} = \mathbf{A}\mathbf{x}_{k+l} + \mathbf{B}\mathbf{u}_{k+l}, \tag{1a}$$

$$\frac{-v_{dc}}{2} \cdot \mathbf{1}_{3\times 1} \leq \mathbf{u}_{k+l} \leq \frac{v_{dc}}{2} \cdot \mathbf{1}_{3\times 1}, \tag{1b}$$

$$-i_{max} \cdot \mathbf{1}_{3\times 1} \leq \mathbf{K}\mathbf{x}_{k+l} \leq i_{max} \cdot \mathbf{1}_{3\times 1}, \tag{1c}$$

where $\mathbf{U}_k = [\mathbf{u}_k^T, \ \cdots, \ \mathbf{u}_{k+N_p-1}^T]^T \in \mathbb{R}^{3\cdot N_p}$ is the complete control input vector, N_p is the prediction horizon, $\mathbf{Q} \geq 0$ and $\mathbf{R} \geq 0$ are weighting matrices, and $\left\|\mathbf{z}\right\|^2_{\mathbf{Q}}$ denotes a 2-norm with the weighting matrix $\mathbf{Q}$. The LCL-filter system dynamic is modeled as shown in (1a) with the detailed derivation of equations and matrices given in [10], [11]. The input constraints based on the available DC-link voltage are given in (1b), and the state constraints of the converter-side currents are given in (1c) with the transformation matrix $\mathbf{K}$ to limit the current in the abc-frame.

TABLE I
System parameters of converter with LC-filter given in [3]

Symbol		Value	Symbol		Value
v_{dc}	Nominal DC voltage	400 V	v_1	Nominal AC voltage (peak)	155 V
S_1	Nominal rated power	3 kVA	f_{sw}	Switching frequency	10 kHz
L_{fi}	Converter-side inductance	2 mH	L_{fg}	Grid-side inductance	4 mH
C_f	Filter capacitance	15 μF	ω_1	Nominal ac angular frequency	314 rad/s

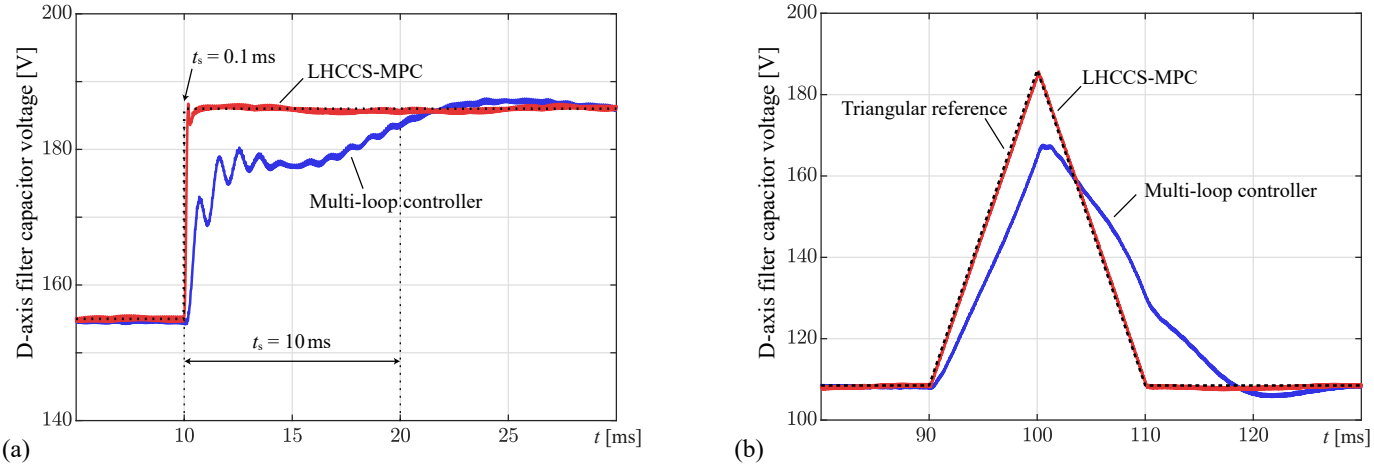

Fig. 3. Comparative simulation results depicting transient responses for different controllers. (a) For a step voltage reference. Reduction of settling time t_s from 10 ms to 0.1 ms. (b) For a triangular ramp voltage reference.

To demonstrate the effectiveness of the proposed method, the control performance of voltage control with the LHCCS-MPC is compared to that of a conventional multi-loop controller. The multi-loop controller is implemented with a PR (proportional-resonant) controller for the voltage loop and a proportional controller for the current loop based on [3]. The LC-filter system parameters used for the simulations are given in table I.

The simulation result for a reference voltage step (20 % of the nominal AC voltage) of the LHCCS-MPC and the multi-loop controller are compared in fig. 3(a). The simulation result of the LHCCS-MPC demonstrates outstanding dynamic control performance with sufficient damping, which reduces the settling time by a factor of approximately 100 compared to the multi-loop controller. Transient responses following a triangular reference voltage of the LHCCS-MPC and the multi-loop controller are compared in fig. 3(b). The comparative simulation results depict superior control performance of MPC as a controllable voltage source following varying references. Therefore, the VSC with an LC-filter can be modeled as a controllable voltage source with minor delay when MPC is used as a voltage controller. In contrast, large time delays and oscillations resulting from the multi-loop controller impair the performance of the controllable voltage source.

Simulation results for a voltage sag and a subsequent recovery with stand-alone operation are shown in fig. 4, where the AC voltage drops to 20 % of the rated value and recovers. Even for such large-signal transients, the simulation results with the LHCCS-MPC demonstrate fast transient behavior with good damping, whereas the multi-mode controller shows large and long oscillations. Furthermore, it can be observed that the LHCCS-MPC effectively avoids over-currents in the

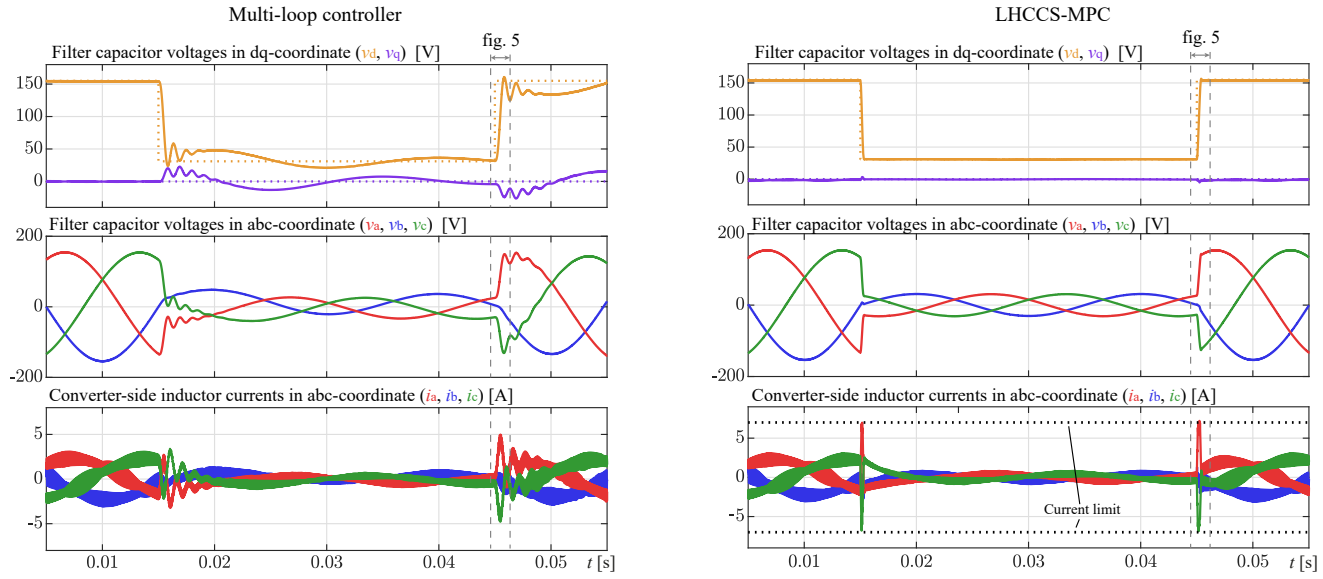

Fig. 4. Comparative simulation results for different controllers during a voltage sag and a recovery in stand-alone operation. The LHCCS-MPC includes state constraints of inductor currents of ±7 A. Typically, the maximum current value is decided based on the current capability of VSCs. However, in this simulation, a lower value is chosen just for a demonstration.

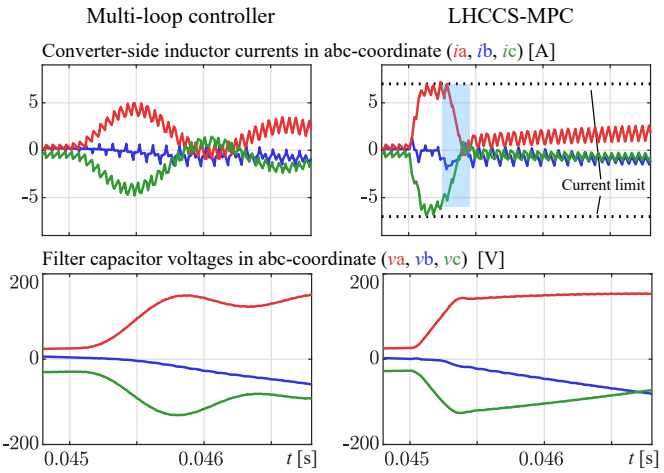

Fig. 5. Magnified simulation results of fig. 4 for comparing the transient behavior. The LHCCS-MPC can forecast the filter capacitor voltages and reduce inductor currents beforehand as highlighted in blue, such that the currents can undergo a seamless transition from the maximum value to the steady-state value with good damping.

converter-side inductor currents with the incorporated state constraints.

The zoomed simulation results during a transient are illustrated in fig. 5. By ramping up the converter-side currents rapidly up to their limits determined by considered state constraints, the LHCCS-MPC can utilise the full dynamic potential for controlling the filter capacitor voltages. Compared to that, the multi-loop controller has a limited control bandwidth and gradually increases the currents, such that the resonance of the LC-filter is not excited.

MPC is capable of achieving a dynamic transient with excellent damping, but only with the utilization of a long prediction horizon. The long horizon enables forecasting of future states, i.e. filter capacitor voltages, and prepares inductor currents to be adapted in advance as the inductor currents cannot be changed instantaneously. To avoid voltage overshoots and oscillations as shown in fig. 5, it is crucial that the inductor currents undergo a seamless transition from a high value, that utilises the system's full dynamic potential, to the required value for steady-state operation, which is highlighted in blue in fig. 5. This adjustment period is critical for achieving the desired level of damping, but cannot be accomplished with short prediction horizon MPC or conventional linear controllers. This is because such controllers cannot forecast the capacitor voltages in advance and the adjustment of the inductor currents can only be performed when the capacitor voltages are already close to the reference values. This limitation results in a suboptimal damping performance or a non-damped behavior with resonances. To avoid this, conventional voltage controllers are typically designed with a low bandwidth to prevent abrupt current changes as shown in fig. 5.

Long prediction horizon brings many benefits to MPC, but the computational burden of MPC increases dramatically with longer prediction horizons. However, recent discoveries in efficient optimisation problem-solving and advances in computational power of embedded systems facilitate a real-time implementation of long-prediction horizon MPC at high sampling rates [12], [13]. Therefore, the proposed method is not just confined to theory or simulation but also can be applied in real converter systems. In the following section, the effects of the proposed dynamic voltage control on the power loop, such as power oscillations, are examined to analyse the influence of the dynamic control on GFMC.

III. Impact of Dynamic Voltage Control using MPC on Grid-forming Control

When a VSC operates as a GFMC, the VSC controls the magnitude V and the angle θ of the filter capacitor voltage at the PCC, which are given as the voltage control references in fig. 2. These references are generated by the power loop, which is responsible for regulating the active P and the reactive Q power transfer via the connected power lines to maintain the required voltage and frequency at the PCC. Many power loop control methods are introduced to control the active P and the reactive Q power via the magnitude V and the angle θ of the filter capacitor voltage [1], [3]. Examples are droop control, virtual synchronous generator, and power synchronization control. Nevertheless, all these methods operate based on the assumption that the filter capacitor voltage control loop has a high control bandwidth and behaves approximately as an ideal controllable voltage source. Therefore, insufficient voltage control performance can deteriorate the decoupling between the P and Q loops and induce power oscillations, which can even cause transient stability problems [5].

As shown in the previous section, the LHCCS-MPC enables a close-to-ideal controllable voltage source with fast voltage control and allows to minimise the coupling of the P and

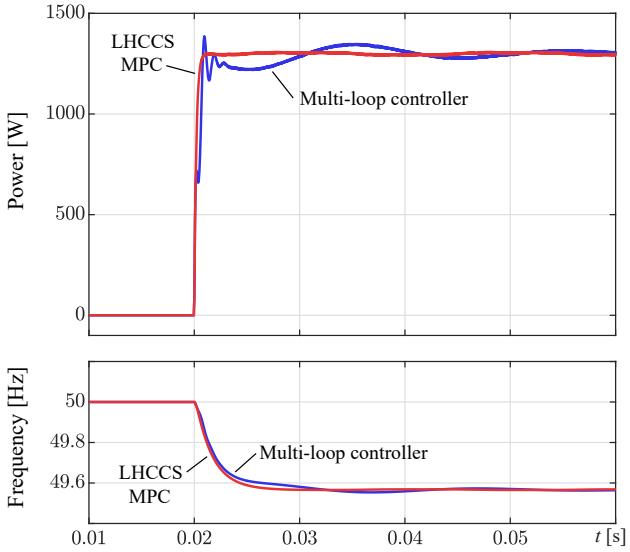

Fig. 6. Comparative simulation results of the power output of the VSC and the frequency output of the P-f droop control for showing the impact of dynamic voltage control on power oscillations.

Q loops and the power oscillations. This section examines the interaction between the power and the voltage control loop and investigates the impact of the dynamic voltage control on the power-loop. Therefore, comparative simulations are conducted with the same power loop control method, but with different voltage control schemes, the LHCCS-MPC and the multi-loop controller. The typical P-f and Q-V droop control with a low-pass filter $G_\mathrm{f} = \omega_\mathrm{f}/(s+\omega_\mathrm{f})$ are adopted, which can be re-formulated in the form

$$\omega_{\mathrm{o,ref}} - \omega_1 = \frac{P_\mathrm{ref} - G_\mathrm{f}\, P}{S_1} \cdot \frac{1}{D_\mathrm{p}}, \tag{2}$$

$$V_{\mathrm{o,ref}} - V_1 = \frac{Q_\mathrm{ref} - G_\mathrm{f}\, Q}{S_1} \cdot \frac{1}{D_\mathrm{q}}, \tag{3}$$

where $\omega_{\mathrm{o,ref}}$ is the angular frequency output of the P-f droop control, P_ref and P are the active power reference and the active power output of the VSC, D_p is the active power droop gain, $V_{\mathrm{o,ref}}$ is the voltage output of the Q-V droop control, Q_ref and Q are the reactive power reference and the reactive power output of the VSC, D_q is the reactive power droop gain. The power loop control parameters are chosen based on [3] $D_p = 50$, $D_q = 10$, $\omega_\mathrm{f} = 628\,\mathrm{rad/s}$, $P_\mathrm{ref} = 0$, $Q_\mathrm{ref} = 0$.

A. Stand-alone Operation with Resistive Load

The simulation results for a stand-alone operation of GFMCs in case of a resistive load step change ($R_\mathrm{load} = \infty \rightarrow 27\,\Omega$) are shown in fig. 7. The resistive load is connected at $t = 0.02\,\mathrm{s}$, and the VSC successfully provides the power to the load with both controllers. Nonetheless, the capacitor voltages and the load currents with the multi-loop controller cause oscillations when the load is connected. In fig.6, the comparative results of the active power output of the VSC and the frequency output are shown to depict the influence of voltage control on power oscillations. The power control with the LHCCS-MPC demonstrates a well-damped power step response, while the result with the multi-loop controller shows oscillations with a larger settling time.

B. Stand-alone Operation with Nonlinear Load

The simulation results for a stand-alone operation of the GFMCs in case of a nonlinear load step change (a 3-phase diode rectifier with a resistive load $R_\mathrm{load} = \infty \rightarrow 81\,\Omega$) are shown in fig. 8. The nonlinear load is connected at $t = 0.02\,\mathrm{s}$, and the currents with high-order harmonics are drawn from the VSCs. The limited control bandwidth of the multi-loop controller results in a significant impact on the quality of the

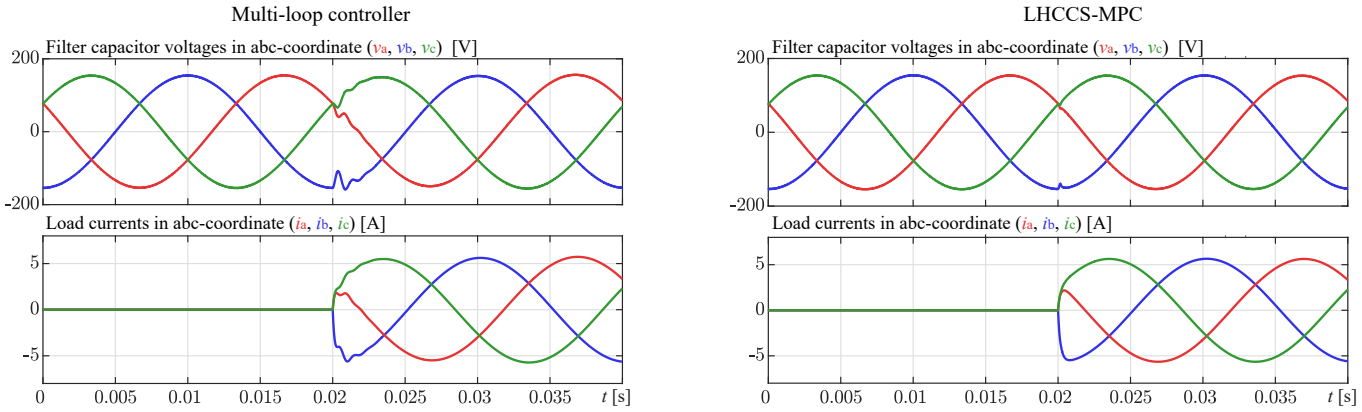

Fig. 7. Comparative simulation results for different controllers for GFMCs in case of a resistive load ($R_\mathrm{load} = 27\,\Omega$) step change.

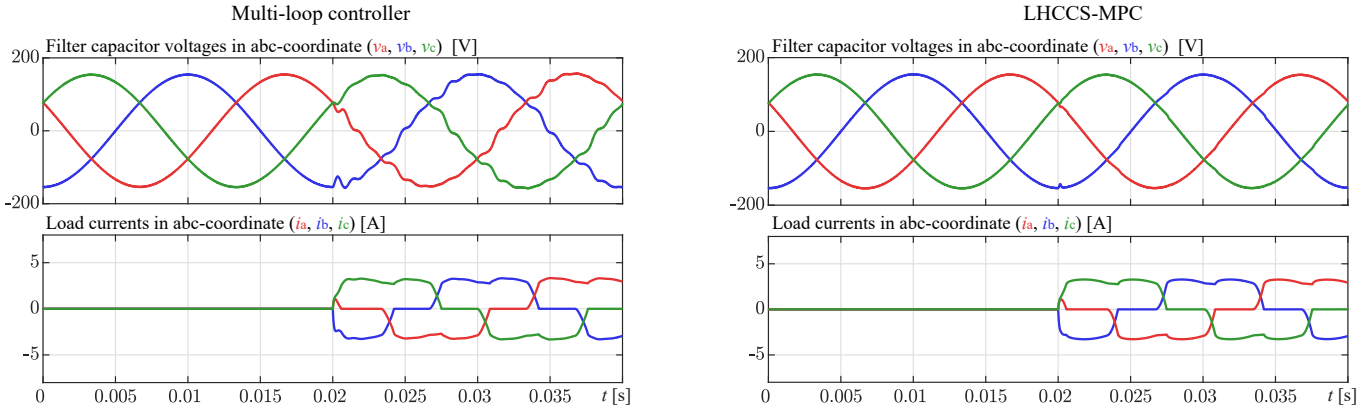

Fig. 8. Comparative simulation results for different controllers for GFMCs in case of a nonlinear load (a 3-phase diode rectifier with a resistive load $R_\mathrm{load} = 81\,\Omega$) step change.

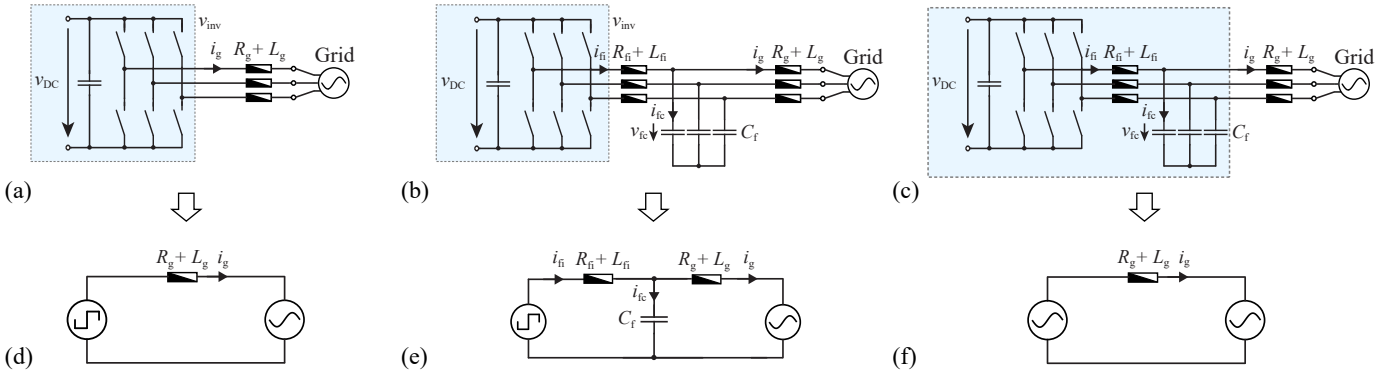

Fig. 9. (a) Conventional VSC with an L-filter using v_{inv} to control i_g. (b) Conventional VSC with an LCL-filter using v_{inv} to control i_g. (c) Proposed VSC with an LCL-filter using v_{fc} to control i_g. (d) Equivalent per-phase phasor model of the VSC with an L-filter. (e) Equivalent per-phase phasor model of the VSC with an LCL-filter. (f) Equivalent per-phase phasor model with an approximated controllable voltage source.

filter capacitor voltages. The resulting high-order harmonic components are clearly visible in the waveforms. In contrast, the LHCCS-MPC achieves filter capacitor voltage waveforms with only low distortions.

The simulation results in this section indicate that the operation of VSCs as GFMCs can greatly benefit from dynamic voltage control. Interestingly, dynamic voltage control can also provide an advantage to VSCs when operating as GFLCs. In the following section, the use of dynamic voltage control to improve the robustness of GFLCs is presented.

IV. Impact of Dynamic Voltage Control using MPC on Grid-following Control

When a VSC with an LC-filter operates as a GFLC, the VSC assumes that the grid is stiff and regulates the injected current level into the grid based on the given grid angle through a PLL. The grid currents become the control objective, and the VSC synthesises the necessary voltages using pulse width modulation (PWM).

Typically, the VSC is controlled directly with a classical linear controller as shown in fig. 9(b). With such a control scheme, LCL-resonances (LC-filter plus grid inductors) challenge the current control, and an extra active damping loop is required for ensuring system stability [14], [15]. However, the damping and the control behavior heavily depend on the system model parameters, and variations in the grid inductance value endanger the system stability and deteriorate the effectiveness of the control [16]. The variations of the grid inductance value are more pronounced in weak grids with connections of parallel converters [16], which are commonly expected in micro-grids and in case of integrating many renewable energy resources in the grid.

By utilising the LHCCS-MPC for the voltage control, the VSC with the output LC-filter can behave like a controllable voltage source with a high bandwidth. This enables a novel operation of the VSC as shown in fig. 9(c). The grid-side current control can be achieved in a similar manner to a simple L-filter current control as shown in fig.9(a). In this case, all control complexities due to resonances and variations in the grid inductance can be avoided, since the L-filter is a first-order system and a robust controller can be easily designed. Naturally, the achievable bandwidth of the GFLC using voltage control is limited. However, with the growing usage of wide-bandgap semiconductors, the required bandwidth for the GFLC can be met for many applications.

Simulation results for variations of the grid inductance, which can occur in parallel inverter based microgrids as shown in [17], are shown in fig. 10. The simulation results with the

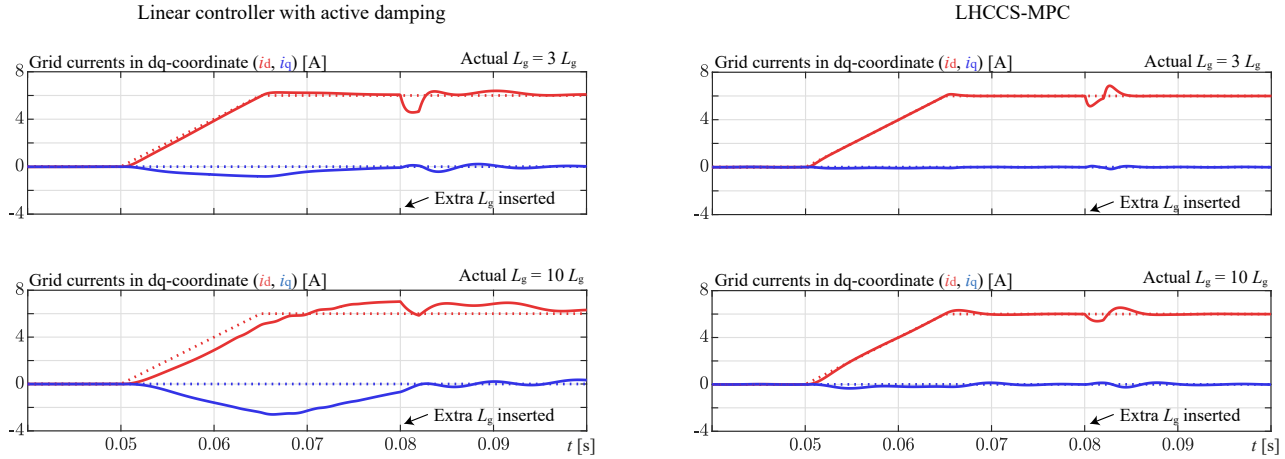

Fig. 10. Comparative simulation results between control schemes in operation as grid-following converters (GFLCs) with varying grid impedance.

LHCCS-MPC demonstrate that the control behavior does not change despite the increment of the inductance value. However, the linear controller with active damping based on [14] shows deteriorated control performance with the increased grid inductance value. The linear controller with active damping can improve the control performance by adjusting control parameters based on grid conditions. However, this approach requires extra control complexity to estimate grid inductances in real-time, and it also poses a risk of instability during parameter transitions.

V. Conclusion

This paper investigates MPC for voltage control of converters with LC-filters and analyses the impact of dynamic voltage control with good damping behavior on the operation as GFMCs or GFLCs. Simulation results for the voltage control show that MPC achieves 100 times faster settling times compared to a conventional multi-loop controller for a step response and enables the converter with LC-filter to be approximately modeled as an ideal controllable voltage source. The dynamic voltage control achieved with MPC enables the operation of GFMCs with reduced power oscillations and lower voltage distortions at the PCC and renders robust operations of GFLCs under varying grid impedances.

Abbreviations

GFLC	Grid-following converter
GFMC	Grid-forming converter
LHCCS-MPC	Long-horizon continuous control set model predictive control
MPC	Model predictive control
PCC	Point of common coupling
PLL	Phase-locked loop
SG	Synchronous generator
VSC	Voltage-source converter

References

[1] D. B. Rathnayake and B. Bahrani, "Multivariable control design for grid-forming inverters with decoupled active and reactive power loops," *IEEE Trans. on Power Electronics*, 2022.

[2] W. Du *et al.*, "A comparative study of two widely used grid-forming droop controls on microgrid small-signal stability," *IEEE Journal of Emerging and Selected Topics in Power Electronics*, vol. 8, no. 2, 2020.

[3] H. Deng, J. Fang, Y. Qi, Y. Tang, and V. Debusschere, "Generic voltage control for grid-forming converters with improved power loop dynamics," *IEEE Trans. on Industrial Electronics*, 2022.

[4] D. Pan, X. Wang, F. Liu, and R. Shi, "Transient stability of voltage-source converters with grid-forming control: A design-oriented study," *IEEE Journal of Emerging and Selected Topics in Power Electronics*, vol. 8, no. 2, 2020.

[5] Y. Liao, X. Wang, and F. Blaabjerg, "Passivity-based analysis and design of linear voltage controllers for voltage-source converters," *IEEE Open Journal of the Industrial Electronics Society*, vol. 1, 2020.

[6] V. Yaramasu, M. Rivera, M. Narimani, B. Wu, and J. Rodriguez, "Model predictive approach for a simple and effective load voltage control of four-leg inverter with an output lc filter," *IEEE Trans. on Industrial Electronics*, vol. 61, no. 10, 2014.

[7] S. Odhano, P. Zanchetta, M. Tang, and C. A. Silva, "MPC using modulated optimal voltage vector for voltage source inverter with LC output filter," in *IEEE Energy Conversion Congress and Exposition (ECCE)*, 2018.

[8] M. Rossi, P. Karamanakos, and F. Castelli-Dezza, "An indirect model predictive control method for grid-connected three-level neutral point clamped converters with LCL filters," *IEEE Trans. on Industry Applications*, 2022.

[9] T. Liu, X. Wang, F. Liu, K. Xin, and Y. Liu, "A current limiting method for single-loop voltage-magnitude controlled grid-forming converters during symmetrical faults," *IEEE Trans. on Power Electronics*, vol. 37, no. 4, 2022.

[10] M. Jeong, T. Gfrörer, and J. Biela, "Extending stable parameter range of LCL-filters for grid-connected converters by inherent damping of model predictive control (MPC)," in *IEEE 23rd Workshop on Control and Modeling for Power Electronics (COMPEL)*, 2022.

[11] C. Fischer, S. Mariéthoz, and M. Morari, "A model predictive control approach to reducing low order harmonics in grid inverters with LCL filters," in *Conf. of the IEEE Ind. Electron. Soc. (IECON)*, 2013.

[12] B. Stellato, G. Banjac, P. Goulart, A. Bemporad, and S. Boyd, "OSQP: an operator splitting solver for quadratic programs," *Mathematical Programming Computation*, vol. 12, no. 4, 2020.

[13] M. Jeong and J. Biela, "When FPGAs meet ADMM with high-level synthesis (HLS): A real-time implementation of long-horizon MPC for power electronic systems," in *11th Int. Conf. on Power Electron. (ICPE - ECCE Asia)*, 2023, in press.

[14] S. G. Parker, B. P. McGrath, and D. G. Holmes, "Regions of active damping control for LCL filters," *IEEE Trans. on Industry Applications*, vol. 50, no. 1, pp. 424–432, 2014.

[15] J. Dannehl, C. Wessels, and F. W. Fuchs, "Limitations of voltage-oriented PI current control of grid-connected PWM rectifiers with LCL filters," *IEEE Trans. on Industrial Electronics*, vol. 56, no. 2, 2009.

[16] R. Peña-Alzola, M. Liserre, F. Blaabjerg, M. Ordonez, and Y. Yang, "LCL-filter design for robust active damping in grid-connected converters," *IEEE Trans. on Industrial Informatics*, vol. 10, no. 4, 2014.

[17] J. He, Y. W. Li, D. Bosnjak, and B. Harris, "Investigation and active damping of multiple resonances in a parallel-inverter-based microgrid," *IEEE Tran. on Power Electronics*, vol. 28, no. 1, 2013.